MITSUBISHI ELECTRIC RESEARCH LABORATORIES
https://www.merl.com

Fingerprinting-Based Indoor Localization with Commercial MMWave WiFi - Part II: Spatial Beam SNRs

Wang, Pu; Pajovic, Milutin; Koike-Akino, Toshiaki; Sun, Haijian; Orlik, Philip V.

TR2019-138 December 09, 2019

Abstract

Existing fingerprint-based indoor localization uses either fine-grained channel state information (CSI) from the physical layer or coarse-grained received signal strength indicator (RSSI) measurements from the MAC layer. In this paper, we propose to use an intermediate channel measurement — spatial beam signal-to-noise ratios (SNRs) that are inherently available during the beam training phase as defined in the IEEE 802.11ad standard — to construct the feature space for location-and orientation-dependent fingerprinting database. We build a 60-GHz experimental platform consisting of three access points and one client using commercial-off-the-shelf routers and collect realworld beam SNR measurements in an office environment during regular office hours. Both position/orientation classification and coordinate estimation are considered using classic machine learning approaches. Comprehensive performance evaluation using real-world beam SNRs demonstrates that the classification accuracy is 99.8% if the location is only interested, while the accuracy is 98.6% for simultaneous position-and-orientations classification. Direct coordinate estimation gives an average root-mean-square error of 17.52 cm and 95% of all coordinate estimates are less than 26.90 cm away from corresponding true locations. This concept directly applies to other mmWave band (e.g., 5G) devices where beam training is also required.

IEEE Global Communications Conference (GLOBECOM)

© 2019 MERL. This work may not be copied or reproduced in whole or in part for any commercial purpose. Permission to copy in whole or in part without payment of fee is granted for nonprofit educational and research purposes provided that all such whole or partial copies include the following: a notice that such copying is by permission of Mitsubishi Electric Research Laboratories, Inc.; an acknowledgment of the authors and individual contributions to the work; and all applicable portions of the copyright notice. Copying, reproduction, or republishing for any other purpose shall require a license with payment of fee to Mitsubishi Electric Research Laboratories, Inc. All rights reserved.

Mitsubishi Electric Research Laboratories, Inc.
201 Broadway, Cambridge, Massachusetts 02139

Fingerprinting-Based Indoor Localization with Commercial MMWave WiFi — Part II: Spatial Beam SNRs

Pu Wang[1], Milutin Pajovic[1], Toshiaki Koike-Akino[1], Haijian Sun[2], and Philip V. Orlik[1]
[1]*Mitsubishi Electric Research Laboratories (MERL), Cambridge, MA 02139, USA*
[2]*Utah State University, Logan, UT, 84322, USA*

***Abstract*—Existing fingerprint-based indoor localization uses either fine-grained channel state information (CSI) from the physical layer or coarse-grained received signal strength indicator (RSSI) measurements from the MAC layer. In this paper, we propose to use an intermediate channel measurement — spatial beam signal-to-noise ratios (SNRs) that are inherently available during the beam training phase as defined in the IEEE 802.11ad standard — to construct the feature space for location-and-orientation-dependent fingerprinting database. We build a 60-GHz experimental platform consisting of three access points and one client using commercial-off-the-shelf routers and collect real-world beam SNR measurements in an office environment during regular office hours. Both position/orientation classification and coordinate estimation are considered using classic machine learning approaches. Comprehensive performance evaluation using real-world beam SNRs demonstrates that the classification accuracy is 99.8% if the location is only interested, while the accuracy is 98.6% for simultaneous position-and-orientations classification. Direct coordinate estimation gives an average root-mean-square error of 17.52 cm and 95% of all coordinate estimates are less than 26.90 cm away from corresponding true locations. This concept directly applies to other mmWave band (e.g., 5G) devices where beam training is also required.**

I. Introduction

WiFi-based indoor localization has received long attraction over the past two decades [1]. Among all frameworks, *fingerprinting-based* method provides an efficient solution for online localization with low computational complexity [2]. On the other hand, it requires enormous time and resources to construct an offline database with chosen fingerprinting features at locations-of-interest to enable fast online localization.

Existing WiFi-based fingerprinting systems have used *received signal strength indicator* (RSSI) as the feature to construct the offline training database due to easy access to commercial 802.11ac devices and low hardware requirements. Machine learning methods such as the k-nearest neighbor (kNN), linear/quadratic discriminant analysis (LDA/QDA), support vector machine (SVM) and decision trees (DT) can be applied to the RSSI-based fingerprinting data and show improved localization accuracy [3], [4]. The common issues of RSSI include 1) instability of RSSI measurements at a given location and 2) coarse-grained channel information.

The use of *channel state information* (CSI) for fingerprinting-based localization gains momentum at 2.4-GHz and 5-GHz frequency bands in [5]–[10] (references therein) due to open-source WiFi network interface cards (NICs) such as Intel WiFi Link 5300 NIC. Specifically, these NICs provide subcarrier channel frequency responses (CFR) in an orthogonal frequency-division multiplexing (OFDM) system and capture the multipath effect via wideband channel responses. Compared with RSSI measurements, these CSI measurements are more stable and provide location-sensitive features. For instance, FIFS leverages the weighted average of CSI amplitudes over three antennas [5], while DeepFi exploits 90 CSI amplitudes from all 30 subcarriers at all three antennas with a deep autoencoder network [7], [8]. To address the firmware problem for phase information, [11] proposed to use CSI phase for angle of arrival (AoA) estimation with 5-GHz WiFi signals. [12] used a capture device to extract the CSI from the CSI feedback step from the user to the access point, converted into so-called angle measurements for fingerprinting data, and applied machine learning algorithms on such fingerprinting data.

For higher frequency bands beyond 5-GHz frequency band, e.g., 28-GHz band for 5G wireless communications and 60-GHz for 802.11ad WiFi [13], obtaining real-world fingerprinting measurements is significantly more challenging and usually requires dedicated prototyping device platforms [14]–[18]. One of unique features of these millimeter-wave (mmWave) applications is to employ high-resolution beampatterns, via either analog beamforming, fully digital beamforming, or hybrid beamforming [19], [20], to compensate for higher path loss at mmWave bands. More specifically, during the so-called beam training phase, a pre-determined set of varying spatial beampatterns is used to probe the environment. For each probing beampattern, a *spatial beam SNR* is recorded and beampatterns with the strongest beam SNR are selected for subsequently transmitting and receiving. For a given probing beampattern, spatial beam SNR is RSSI-like coarse-grained channel measurement. However, with multiple varying beampatterns, a set of spatial beam SNRs embed more spatial channel responses than the traditional RSSI measurement. Furthermore, spatial beam SNRs are inherently available in the 5G and IEEE 802.11ad standard, that enables zero overhead for the overall hardware and software infrastructure.

The use of beam information in mmWave frequency bands has been considered in the past for indoor localization in [21], [22] and references therein. Particularly, [21] proposed a direct localization (as opposed to the fingerprinting-based approach) with particle filters along with linear programming and Fourier analysis to real-world beam SNR measurements from commercial-off-the-shelf (COTS) 60-GHz WiFi routers. Another related work is to use two-dimensional power delay

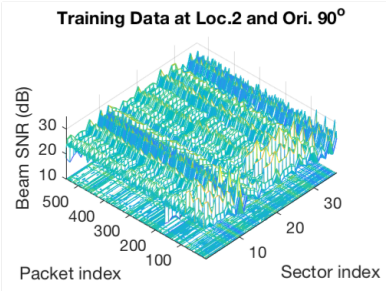

Fig. 1: Real-world spatial beam SNR measurements at one AP using a commercial 802.11ad device in an office environment, where 36 irregular beampatterns (sector index) are used by the device to report 36 beam SNR values for a packet.

profile (PDP) over multiple beampatterns as fingerprints at 28-GHz band for outdoor localization [22]. It mainly exploits the fact that users' locations can be registered by multipath delays due to surrounding obstructions (e.g., buildings and trees). To obtain high-resolution PDP, it assumes that base stations transmit short pulses with a sequence of directive beamforming patterns and a high sample rate is required at the user to separate closely-spaced delays. Moreover, this concept was verified only using ray-tracing simulated datasets.

As opposed to using the two-dimensional PDP in [22] that requires additional hardware modifications, this paper proposes to use *spatial beam SNRs*[1], conveniently available during the beam training phase in the 5G and 802.11ad standards, as location-and-orientation-depdenent fingerprints with zero overhead. Based on the open source software framework [24] to extract 60-GHz beam SNR measurements, we build an experimental platform consisting of multiple access points (APs) and collect comprehensive indoor measurements in an office environment during regular office hours. Note that these real-world measurements account for hardware constraints such as quantization of beam SNR values (i.e., beam SNRs are acquired at a resolution of 0.25 dB) and non-ideal system factors such as irregular antenna beampatterns.

With these real-world beam SNR measurements at several locations-of-interest, we construct a fingerprinting dataset in the offline training phase. For the online localization phase, both position-and-orientation classification and coordinate estimation are considered using, among classic machine learning approaches, the (weighted) nearest neighboring (NN) and Gaussian process (GP) regression approaches. Comprehensive performance evaluation using real-world beam SNRs demonstrates that we can achieve an accuracy of 98.6% for simultaneously localizing 7 positions with a sub-meter separation and 4 orientations that are $90°$ apart, while conventional approaches using RSSI-like single-SNR measurements offer an accuracy around 40%. If location is the only interest, the accuracy increases to 99.8% for using spatial beam SNRs, which is significantly higher than the accuracy around 54% for using single-SNR measurements. The beam SNR-based fingerprinting localization also shows robustness when the test data were collected at several off-grid locations that are different from those used for training data. In this case, the coordinate estimation with the Gaussian process method gives an average root-mean-square error (RMSE) of 17.52 cm and 95% of all coordinate estimates are less than 26.90 cm away from their true locations.

[1]Separately, Part-I of this work [23] proposes to use RSSI along with beam indices for fingerprinting-based indoor localization.

II. Fingerprinting-Based Indoor Localization with Beam SNR Measurements

In the following, we introduce the beam SNRs, a type of zero-overhead measurement available in the 802.11ad standard. The beam SNRs feature is a coarse-grained channel measurement but carries rich information on spatial propagation paths, for fingerprinting-based indoor localization.

A. Beam SNRs Measurements from 802.11ad Devices

To compensate for higher path loss in mmWave bands, IEEE 802.11ad standards use directional antenna beampatterns to focus transmitting energy on a desired direction. To search for this desired direction, a series of pre-defined beampatterns or sectors are used by APs to send beacon messages to potential clients which in a listening mode with a quasi-ominidirectional beampattern. Then, clients send a series of beampatterns while the APs are in a listening mode. After the sector sweeping, the connection can be established by choosing the pair of beam sectors by the AP and user. Such sector sweep is periodically repeated and the beam sectors are updated to adapt to the environmental changes. As a result, the beam SNR measurements from multiple beam sectors are inherently available from 802.11ad devices without any overhead. As one of commercial 60-GHz WiFi devices, TP-Link AD7200 router uses a phased array of 32 antenna elements to send 36 pre-defined directional beampaterns. Due to the antenna housing and calibration, irregular antenna beampatterns are effectively formed in the phased array [21].

Given the antenna beampatterns, the beam SNR for the mth beampattern is defined as

$$h_m = \text{Beam SNR}_m = \frac{1}{\sigma^2} \sum_{i=1}^{I} \gamma_m(\theta_i) P_i(\theta_i), \qquad (1)$$

where I is the total number of paths, θ_i is the azimuth angle for the ith path, $P_i(\theta_i)$ is the signal power at the ith path, $\gamma_m(\theta_i)$ is the mth antenna beampattern gain at the ith path, and σ^2 is the noise variance. For TP-Link AD7200 routers, the beam SNRs are recorded in a stepsize of 0.25 dB.

B. Offline Training Dataset

To construct the fingerprinting dataset, we stack all SNR measurements from all beam sectors as a vector, e.g., $\mathbf{h} = [h_1, h_2, \ldots, h_M]^T$ with $[\cdot]^T$ denoting the transpose. When multiple APs are used, we combine beam SNR measurements from each AP to form one fingerprinting snapshot, i.e., $\tilde{\mathbf{h}} = [\mathbf{h}_1^T, \mathbf{h}_2^T, \ldots, \mathbf{h}_P^T]^T \in \mathbb{R}^{MP \times 1}$, where P is the number of APs. For a given location and orientation, R fingerprinting snapshots, $\tilde{\mathbf{h}}_1(l,o), \cdots, \tilde{\mathbf{h}}_R(l,o)$, are collected to construct the

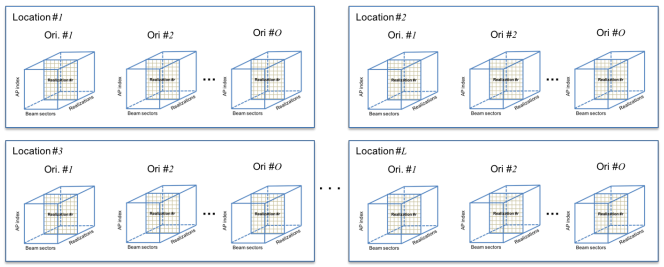

Fig. 2: Constructing offline training datasets with beam SNRs measured at L locations and O orientations.

offline training dataset, where l and o are the indices for the location and orientation, respectively.

Fig. 1 shows an example of real-world beam SNR measurements at one AP using the commercial TP-Link AD7200 router in an office environment, where $M = 36$ beam sectors are swept to measure SNRs. It is seen that the beam SNR patterns remain stable over time (packet index) with a few fluctuations at some packet indices. The distinct pattern over the beam index is the fingerprinting feature we capture in the training dataset. By collecting many realizations of beam SNR measurements at multiple APs over L locations-of-interests and O orientations, we will have LO sets of $MP \times R$ beam SNR measurements in the training dataset. The training dataset is illustrated in Fig. 2.

C. Online Localization Using Spatial Beam SNRs

When new fingerprinting measurements from an unknown location are available, the problem of interest is to, with a chosen performance metric, find the best match of the new measurements in the offline training dataset and determine its location. In the following, we introduce the NN and GP algorithms for classification and coordinate estimation.

1) Position/Orientation Classification: One simple approach to classify new fingerprinting measurements into one of training locations is the kNN method. The kNN method relies on a metric of distance, e.g., Euclidean distance and Minkowski distance of ℓ_p norms, between the beam SNR measurements. A decision is made by examining the labels on the k nearest neighbors with respect to new fingerprinting measurements and taking a vote. Specifically, we define the distance metric between two beam SNR vectors as follows

$$d(\mathbf{h}, \mathbf{h}') = \sqrt{\frac{1}{M}(\mathbf{h} - \mathbf{h}')^T \mathbf{W} (\mathbf{h} - \mathbf{h}')}, \tag{2}$$

where $\mathbf{W}$ is a diagonal matrix with diagonal elements denoting the importance of corresponding beam sectors. This weighted distance metric can be straightforwardly extended to the case of multiple SNR measurements and multiple APs.

We first train the kNN classification model based on all beam SNR measurements in the training data in Fig. 2 with both location and orientation labels. Then, for a candidate location and orientation, we collect a batch of Q beam SNR snapshots, $\bar{\mathbf{h}}_1, \cdots, \bar{\mathbf{h}}_Q$, and compute the batch of all Q test snapshots with a window of Q measurements sliding through the training dataset

$$d_t(l,o) = \sqrt{\frac{\sum_{q=1}^{Q} (\tilde{\mathbf{h}}_{t+q-1}(l,o) - \bar{\mathbf{h}}_q)^T \mathbf{W} (\tilde{\mathbf{h}}_{t+q-1}(l,o) - \bar{\mathbf{h}}_q)}{MQ}}, \tag{3}$$

where $t = 1, \ldots, R - Q + 1$, $l = 1, \cdots, L$ and $o = 1, \ldots, O$. From all $(R - Q + 1)LO$ computed distances, the k nearest samples are selected and, from their labels of locations and orientations, the most frequently appeared label is picked as the predicted label for the candidate location and orientation. When $k = 1$, the location and orientation are determined by choosing the one giving the smallest distance:

$$(\hat{l}, \hat{o}) = \arg\min_{l,o} \left[\min_{t=1,\cdots,R-Q+1} d_t(l,o) \right]. \tag{4}$$

When only the location is of interest, we can simply repeat the above process by only using the location label from the training dataset. Similarly, one can apply other classification methods to the beam SNR measurements. In Section. III-C, we will evaluate localization performance of various classification methods on real-world beam SNR measurements collected in an office environment.

2) Coordinate Estimation: We can also estimate coordinates of test locations using fingerprinting datasets. One widely used approach is the weighted kNN method which uses a weighted mean of the coordinates of k nearest training locations as the estimated coordinates. The weight coefficients are computed using the Euclidean distance in the feature space. In this paper, due to multiple orientations at a given location and a limited number of training locations, we adopt a weighted kNN method directly on the beam SNR measurement space. Specifically, the above classification step obtains the smallest k distances between the new measurement and the training dataset. For each of the k beam SNR measurements in training data, we compute the distance $\{d_i\}_{i=1}^{K}$ as (3). Then the coordinates of test data are estimated as follows

$$(\hat{x}, \hat{y}) = \frac{\sum_{i=1}^{k} w_i \times (x_i, y_i)}{\sum_{i=1}^{K} w_i}, \tag{5}$$

where (x_i, y_i) is the coordinate of training locations with the k smallest distances, and w_i is the corresponding weight determined by $w_i = \gamma/d_i + \varepsilon$ with ϵ is a small positive number to prevent the denominator from zero and γ is a normalized parameter.

It it noted that the weighted kNN method still relies on the classification results. Instead, we can directly estimate the coordinate of test locations by directly formulating the coordinate estimation as a supervised regression problem from the multi-AP beam SNR measurements to two-dimensional (2-D) coordinates. Specifically, we first apply the GP with a choice of kernel function (e.g., exponential and radial-basis function) to labeled fingerprinting data at training locations. A

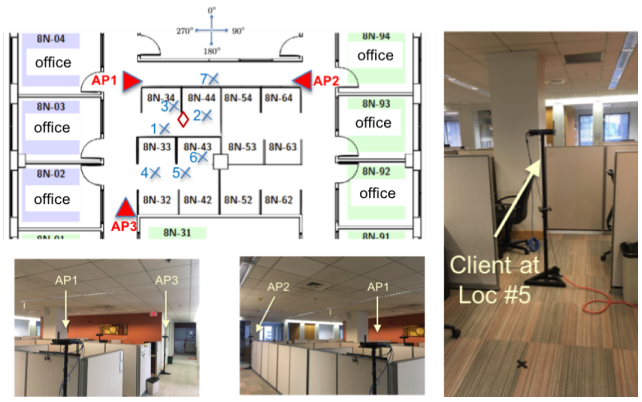

Fig. 3: Experimental setup with 3 APs (denoted by triangles) in 7 locations-of-interest (denoted by crosses) in an office environment.

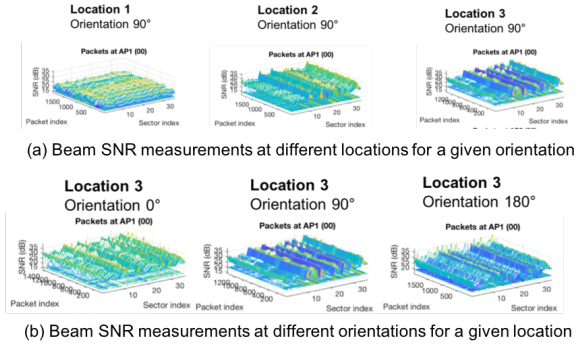

(a) Beam SNR measurements at different locations for a given orientation

(b) Beam SNR measurements at different orientations for a given location

Fig. 4: Spatial beam SNR measurements at AP1 when the client is positioned at a) three locations with the same orientations; and b) the same location but with different orientations.

set of hyperparameters of the chosen kernel is optimized with beam SNR measurement as input and training coordinates as output by maximizing the log marginal-likelihood (ML) with an equally likely prior on all training locations. Then, the direct coordinate estimation is obtained by applying the optimized GP to the new beam SNR measurement.

III. Indoor Experiment

In the following, we evaluate the fingerprinting-based indoor localization with beam SNR measurements collected from a testbed platform in an office environment during office hours.

A. Testbed Platform

The testbed consists of four 802.11ad devices, three serving as APs and one serving as the client, in a configuration shown in Fig. 3. These 4 devices are connected via wire cables to a workstation to allow configurations of the role of each device and to access the beam SNR measurements. Particularly, we chose Talon AD7200 routers that use a Qualcomm QCA9500 60 GHz chipset that comes with a phased antenna array of 32 antenna elements and fully implements the IEEE 802.11ad standard. During the beam training phase, a total number of 36 predefined antenna patterns are swept by changing the weights in the antenna elements. When the router is in reception mode, quasi omni-directional antenna pattern is used.

To access the raw beam SNR measurements, we follow the work in [21], [25], [26] and used the open-source software package in [24]. Particularly, we used the Nexmon firmware patching framework [27], which enables the development of binary firmware extensions in C.

B. Experiment Configuration

The testbed is deployed in an office environment during office hour, as shown in Fig. 3. There are 6 offices on both sides and 8 cubicles in the middle. All 6 offices and 4 cubicles on the right are occupied by staff. Furniture including chairs, tables, desktops are present in the cubicles.

These 3 APs, denoted as red triangles, are fixed in the aisle with fixed orientations. Specifically, AP1, AP2 and AP3 point to $90°$, $180°$ and $0°$, respectively, where the orientation reference is marked out in Fig. 3. To collect fingerprinting training data, we position the client at one of 7 locations-of-interest marked by crosses in Fig. 3. At each of the 7 locations, we collect beam SNR measurements by rotating the client to 4 orientations at $[0°, 90°, 180°, 270°]$. Overall, the offline training dataset consists of beam SNR measurements from $L = 7$ locations and $O = 4$ orientations.

Samples of the collected data at AP1 are shown in Fig. 4. It is seen from Fig. 4 that all beam SNR measurements are stable over time (packet index) with only a few fluctuations at a few packets, possibly due to people moving. On the other hand, the measurements are sensitive to the client's position and orientation as beam SNRs change more rapidly over beam indices.

IV. Performance Evaluation

A. Location and Orientation Classification

In this section, we present our results for the fingerprinting-based localization system. For this purpose, we use the confusion matrix as the performance metric for position and orientation classification

$$\mathbf{C}(i,j) = \frac{1}{T_i} \sum_{t=1}^{T_i} \mathbb{1}[\hat{l}(\tilde{\mathbf{h}}_t(j)) = i], \tag{6}$$

where i and j are indices, respectively, for the estimated and true locations/orientations, T_i is the number of sample batches in the test dataset, and $\mathbb{1}(\cdot)$ is the indicator function

TABLE I: Number of training (test) samples for each location and orientation.

Loc. / Ori.	0°	90°	180°	270°
1	417 (480)	594 (549)	562 (361)	560 (326)
2	572 (140)	546 (302)	582 (176)	402 (224)
3	207 (319)	267 (253)	565 (328)	428 (299)
4	520 (204)	510 (192)	453 (167)	129 (223)
5	511 (287)	498 (322)	396 (307)	118 (303)
6	507 (427)	419 (220)	300 (190)	281 (156)
7	530 (199)	210 (72)	413 (139)	510 (196)

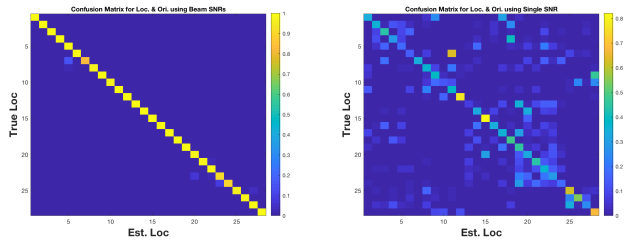

(a) Beam SNRs (b) Single SNR

Fig. 5: Confusion matrices for *simultaneous position-and-orientation* classification using the kNN method ($k = 3$). Indices represent 28 combinations of 7 positions and 4 orientations.

TABLE II: Impact of Classification Methods

	Location + Orientation		Location Only	
	Single SNR	Beam SNRs	Single SNR	Beam SNRs
LDA	**41.1**%	96.2%	47.7%	**100**%
QDA	41.0%	92.3%	**54.2**%	**100**%
SVM	39.9%	96.7%	54.1%	99.7%
DT	31.3%	72.1%	46.1%	91.7%
1NN	33.2%	98.5%	46.7%	99.9%
3NN	35.6%	**98.6**%	48.1%	99.8%

which equals 1 when the argument is true or 0 otherwise. In addition, $\hat{l}(\tilde{\mathbf{h}}_t(j))$ is the location/orientation estimate by using the tth sample batch from the test data collected at jth location/orientation. To evaluate the classification performance, we collected *independent* test datasets at the same 7 locations with 4 orientations on a different date, where the number of test data is shown in parentheses of Table I.

1) Beam SNRs versus Single SNR: Fig. 5 compares the confusion matrix using the kNN method of $k = 3$ with a) beam SNR measurements and b) single SNR (RSSI-like) measurements. Particularly, we extract only one SNR measurement (from the highest average SNR) from all 36 beam SNRs at each AP. It is clear to conclude from Fig. 5 that the kNN method is able to localize both position and orientation accurately by using spatial beam SNRs. Specifically, a classification accuracy of 98.55% is achieved on average by the kNN method with beam SNRs, whereas the kNN method with the single SNR offers an average success rate of 35.6%. For location-only classification, using spatial beam SNRs can significantly improve the classification accuracy from 48.1% of the single SNR case to 99.81%.

TABLE III: Classification accuracy for different combinations of APs using independent test dataset

APs		Location + Orientation	Location Only
1 AP	AP1	83.27%	98.19%
	AP2	84.85%	92.88%
	AP3	81.26%	90.51%
2 APs	AP1 + AP2	97.50%	99.26%
	AP1 + AP3	91.98%	99.59%
	AP2 + AP3	93.00%	97.53%
All 3 APs		98.55%	99.81%

2) Impact of Classification Methods: To evaluate the impact of classification methods, we apply other classical machine learning methods, namely LDA, QDA, SVM and DT methods, to the same training and test datasets used by the kNN method. The results are shown in Table III. Overall, we observe that 1) classification using beam SNRs significantly improves the classification accuracy over that using single SNR and 2) all classification methods except the DT show comparable performance for both simultaneous location-and-orientation and location-only classifications.

3) Impact of the Number of APs: Next, we evaluate the localization performance by using single AP or combinations of 2 APs. The classification accuracy is shown in Table III. When only one AP is used, the success probabilities of simultaneous location-and-orientation classification can reach at 83.27%, 84.85% and 81.26%, respectively, for AP1, AP2 and AP3. When one more AP is available, the probabilities of successful determination is increased to 97.50%, 91.98% and 93.00%, respectively. The best performance is achieved by using all three APs. Similar observation can be made for the location-only classification.

B. Coordinate Estimation

In practice, it is unlikely that the test data are collected at the same location or orientation in the training dataset. Therefore, we next evaluate the performance of coordinate estimation using 4 off-grid test locations, as shown as Loc-A/B/C/D in green squares in Figs. 6 (a) and (b). The test dataset at 4 off-grid locations was collected 4 month later than the fingerprinting training dataset collected in 7 fingerprinting locations.

We apply the weighted kNN method and the GP-based regression method as detailed in Section II-C.2) to the off-grid test dataset. Figs. 6 (a) shows the distribution of coordinate estimates for the GP method (Corresponding results for the weighted kNN method are skipped due to page limit). It is seen that the GP method gives clustered estimates around true positions. It is notable that the coordinate estimates at Loc-D are biased to the right, while the estimates at Loc-C are more centered at Loc-C. By computing distances between these estimates and the true locations, we plot the cumulative distribution function (CDF) in Fig. 6 (b) for estimation distance errors for all 4 off-grid locations for the GP method. It is found that he GP method gives an average RMSE of 17.52 cm, while the weighted kNN shows an average RMSE of 27.18 cm. Out of all coordinate estimates at these 4 test locations, 95% of them are less than 26.90 cm away from corresponding true locations.

V. Conclusions

To the best of our knowledge, our study is the first-of-its-kind to use spatial beam SNRs, collected during the beam training phase from commercial 802.11ad devices, to construct the offline fingerprinting database. This concept also applies to mmWave band 5G devices where beam training is also required. With a multi-AP testbed in an indoor office

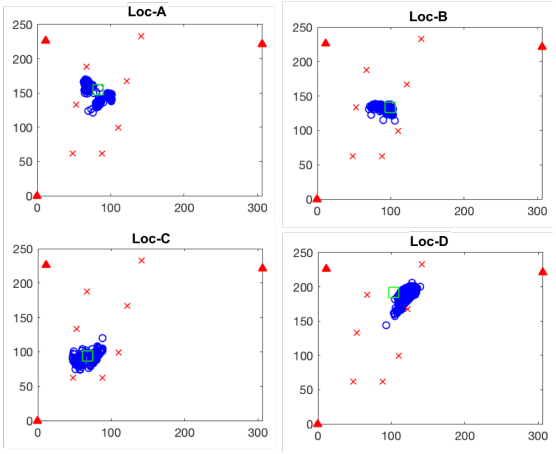

(a) Estimated coordinate (GP)

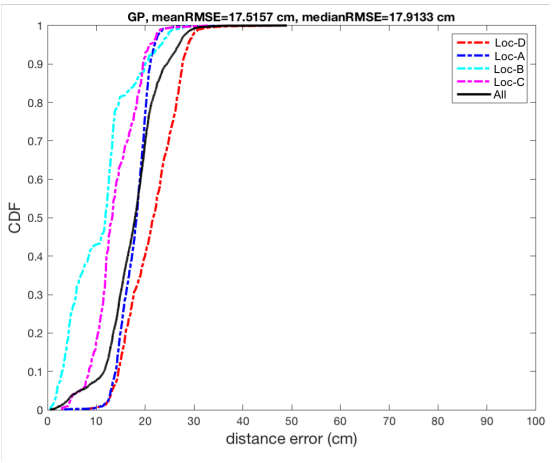

(b) CDF (GP)

Fig. 6: Coordinate estimates (blue circles) at 4 off-grid test locations (referred to as Loc-A/B/C/D in green squares) for the GP method and corresponding CDF curves. The horizontal and vertical axes denote, respectively, the x-axis and y-axis in cm.

environment, localization performance was evaluated by considering various factors such as the number of training data, different combinations of access points, and various machine learning algorithms. The classification accuracy is 98.6% for simultaneous location-and-orientation classification and above 99.8% for location-only classification. The robustness of direct coordinate estimation was tested when the test data were collected at several off-grid locations. Next, we plan to further exploit deep-learning approaches for direct coordinate estimation and evaluate the impact of the blockage of human body on the localization performance.

REFERENCES

[1] H. Liu, H. Darabi, P. Banerjee, and J. Liu, "Survey of wireless indoor positioning techniques and systems," *IEEE Transactions on Systems, Man, and Cybernetics, Part C*, vol. 37, no. 6, pp. 1067–1080, Nov 2007.

[2] P. Bahl and V. N. Padmanabhan, "RADAR: an in-building RF-based user location and tracking system," in *Proceedings IEEE INFOCOM 2000*, March 2000, vol. 2, pp. 775–784.

[3] M. Youssef and A. Agrawala, "The Horus location determination system," *Wirel. Netw.*, vol. 14, no. 3, pp. 357–374, June 2008.

[4] Z. Wu et. al., "Location estimation via support vector regression," *IEEE Trans. on Mobile Computing*, vol. 6, no. 3, pp. 311–321, March 2007.

[5] J. Xiao, K. Wu, Y. Yi, and L. M. Ni, "FIFS: Fine-grained indoor fingerprinting system," in *2012 ICCCN*, July 2012, pp. 1–7.

[6] K. Wu et. al., "CSI-based indoor localization," *IEEE Trans. on Parallel and Distributed Systems*, vol. 24, no. 7, pp. 1300–1309, July 2013.

[7] X. Wang, L. Gao, S. Mao, and S. Pandey, "DeepFi: Deep learning for indoor fingerprinting using channel state information," in *IEEE WCNC*, March 2015, pp. 1666–1671.

[8] X. Wang, L. Gao, S. Mao, and S. Pandey, "CSI-based fingerprinting for indoor localization: A deep learning approach," *IEEE Transactions on Vehicular Technology*, vol. 66, no. 1, pp. 763–776, Jan 2017.

[9] C. Chen, Y. Chen, Y. Han, H. Lai, F. Zhang, and K. J. R. Liu, "Achieving centimeter-accuracy indoor localization on WiFi platforms: A multi-antenna approach," *IEEE Internet of Things Journal*, vol. 4, no. 1, pp. 122–134, Feb 2017.

[10] H. Chen, Y. Zhang, W. Li, X. Tao, and P. Zhang, "ConFi: Convolutional neural networks based indoor Wi-Fi localization using channel state information," *IEEE Access*, vol. 5, pp. 18066–18074, 2017.

[11] J. Gjengset et. al., "Phaser: Enabling phased array signal processing on commodity wifi access points," in *ACM Mobicom*, Sep. 2014, pp. 153–164.

[12] T. Fukushima et. al., "Evaluating indoor localization performance on an IEEE 802.11ac explicit-feedback-based CSI learning system," in *2019 IEEE GLOBECOM*, Dec. 2019 VTC Spring.

[13] "Part 11: Wireless LAN mac and phy specifications amendment 3: Enhancements for very high throughput in the 60 GHz band," *IEEE Std 802.11ad-2012*, pp. 1–628, Dec 2012.

[14] M. Samimi et. al., "28 GHz angle of arrival and angle of departure analysis for outdoor cellular communications using steerable beam antennas in New York city," in *2013 VTC Spring*, June 2013, pp. 1–6.

[15] H. Zhao et. al., "28 GHz millimeter wave cellular communication measurements for reflection and penetration loss in and around buildings in New York city," in *2013 IEEE ICC*, June 2013, pp. 5163–5167.

[16] Y. Azar et. al., "28 GHz propagation measurements for outdoor cellular communications using steerable beam antennas in New York city," in *2013 ICC*, June 2013, pp. 5143–5147.

[17] O. Salehi-Abari et. al., "Millimeter wave communications: From point-to-point links to agile network connections," in *HotNets*, 2016.

[18] B. Ai et. al., "On indoor millimeter wave massive MIMO channels: Measurement and simulation," *IEEE Journal on Selected Areas in Communications*, vol. 35, no. 7, pp. 1678–1690, July 2017.

[19] T. S. Rappaport et. al., "Millimeter wave mobile communications for 5G cellular: It will work!," *IEEE Access*, vol. 1, pp. 335–349, 2013.

[20] R. Méndez-Rial, C. Rusu, N. González-Prelcic, A. Alkhateeb, and R. W. Heath, "Hybrid MIMO architectures for millimeter wave communications: Phase shifters or switches?," *IEEE Access*, pp. 247–267, 2016.

[21] G. Bielsa et. al., "Indoor localization using commercial off-the-shelf 60 GHz access points," in *IEEE INFOCOM 2018*, April 2018, pp. 2384–2392.

[22] J. Gante, G. Falcão, and L. Sousa, "Beamformed fingerprint learning for accurate millimeter wave positioning," in *2018 VTC Fall*, Aug 2018.

[23] M. Pajovic, P. Wang, T. Koike-Akino, H. Sun, and P. V. Orlik, "Fingerprinting-based indoor localization with commercial MMWave WiFi routers - Part I: RSS and Beam Indices," in *2019 IEEE Global Communications Conference (GLOBECOM)*, Dec. 2019, submitted.

[24] D. Steinmetzer, D. Wegemer, and M. Hollick, "Talon tools: The framework for practical IEEE 802.11ad research," in *Available: https://seemoo.de/talon-tools/*, 2018.

[25] D. Steinmetzer, D. Wegemer, M. Schulz, J. Widmer, and M. Hollick, "Compressive millimeter-wave sector selection in off-the-shelf IEEE 802.11ad devices," in *CoNEXT 2017*, December 2017.

[26] S. K. Saha et. al., "Fast and infuriating: Performance and pitfalls of 60 GHz WLANs based on consumer-grade hardware," in *SECON'18*, June 2018.

[27] M. Schulz, D. Wegemer, and M. Hollick, "Nexmon: The c-based firmware patching framework," in *Available: https://nexmon.org*, 2017.